Optimal Glideslope Guidance Algorithm for Minimum-Fuel Fixed-Time Elliptic Rendezvous

Yassine Ariba, Denis Arzelier, Laura Sofia Urbina

Optimal Glideslope Guidance Algorithm for Minimum-Fuel Fixed-Time Elliptic Rendezvous

Yassine Ariba [*,**], **Denis Arzelier** [**], **Laura Sofia Urbina** [**],

[*] *ICAM, 75 avenue de Grande Bretagne, 31300 Toulouse, France (email: yassine.ariba@icam.fr)*
[**] *CNRS, LAAS, 7 avenue du colonel Roche, F-31400 Toulouse, France and Univ de Toulouse, LAAS, F-31400 Toulouse, France (e-mails: yassine.ariba@laas.fr, arzelier@laas.fr, lsurbina@laas.fr).*

Abstract: This paper presents a new minimum-fuel glideslope guidance algorithm for approaching autonomously a target evolving on an elliptic orbit. In addition to the usual rectilinear profile to follow as in Hablani's seminal paper, two new features are requested for the new algorithm. The first one imposes bounds on the guidance error inherent to chemical propulsion glideslope guidance, such that the chaser's trajectory does not escape from an admissible domain. The second one minimizes the consumption during rendezvous. Indeed, unlike the classical glideslope algorithm for which there is no direct control on the fuel consumption, additional degrees of freedom and relevant decision variables may be identified. By combining a useful parametrization of the Tschauner-Hempel relative equations of motion and results from polynomial optimization, a semidefinite formulation of the constraints on the maximal guidance error is obtained. For a fixed-time glideslope rendezvous with a pre-assigned number of maneuvers, a fuel-optimal solution with a bounded guidance error is obtained by solving a semidefinite programming problem. Two numerical examples illustrate the usefulness of the method compared to the classical ones when the approach corridor has to verify stringent geometrical restrictions such as line-of-sight constraints.

Keywords: Glideslope approach, impulsive control, elliptic rendezvous, Tschauner-Hempel equations, semidefinite programming

1. INTRODUCTION

Rendezvous (RDV) between two spacecraft (a target and a chaser) has been one of the most salient operational technology since its first manual achievement in the sixties between a Gemini vehicle and an unmanned target vehicle. Recently, an increasing demand is witnessed to perform autonomous rendezvous, proximity or On-Orbit Servicing operations between an active chaser spacecraft and a passive target spacecraft. Autonomy means that appropriate RDV guidance schemes should combine the simplicity of onboard implementation and a low level of fuel consumption. If the closing phase of the complete rendezvous process is particularly concerned, the assumption that the distance between the chaser and the target is small enough compared to the distance between the target and the center of attraction means that a linearized model for relative dynamics may be used to simplify the design of guidance schemes. The objective of the closing phase is to steer the chaser from several kilometers to few hundreds of meters near the orbital target applying short high thrust pulses approximated as impulsive maneuvers. This idealization of the real actuation may greatly simplify the design of efficient guidance schemes for close range rendezvous operations (Fehse (2003)). The impulsive approximation consists of instantaneous velocity increments which are applied to the actuated spacecraft whereas its position remains unchanged.

This paper focuses on the fixed-time linearized minimum-fuel impulsive closing phase rendezvous problem. Depending on various operational and safety constraints, various closing phase strategies may be envisioned and proposed to realize the proximal rendezvous: V-bar (curvilinear orbit direction as a straight line) and R-bar (direction of the center of attraction) are very classical approaches while looping trajectory or natural drift orbit to R-bar approach are interesting variations as described by Fehse (2003). Observability (line-of-sight constraints), safety reasons and fuel budget are the main incentives to make a choice among all possible approaches. One simple and general scheme complying to safety restrictions is known as the glideslope approach. This trajectory is a straight path in any direction connecting the current location of the chaser to its final destination. The glideslope approach has been first defined in the past for rendezvous and proximity operations involving the space shuttle, Pearson (1989). This preliminary study has been extended and generalized later for any direction in space and circular reference orbit in Hablani et al. (2002), Wang et al. (2007) and for elliptic reference orbit in Okasha and Newman (2011). Indeed, the results presented in Hablani et al. (2002) are well-known and define the so-called classical glideslope algorithm.

Our goal is to extend a previous work from Ariba et al. (2016) where the classical glideslope algorithm of Hablani was revisited in specific cases (V-bar and R-bar approaches) to the general setup and for an elliptic reference orbit. The objective is to identify a new formulation of the problem including useful degrees of freedom that allows to minimize the fuel consumption and helps to enclose the resulting trajectory segments between two successive maneuvers, usually referred to as hopping, in a user-defined approach corridor. Indeed, combining a suitable parametrization of the Tschauner-Hempel relative equations of motion and results from polynomial optimization, a semidefinite programming problem is obtained and propose a minimum-fuel solution to the glideslope guidance problem while controlling the guidance error. The pro-

posed algorithm is compared to the classical glideslope algorithm on two numerical examples, illustrating the interest of this new approach in terms of consumption reduction and admissibility of the trajectory in a corridor of visibility. Note that the trajectories are considered in an open-loop setup in this paper whereas real trajectories undergo orbital disturbances and therefore, have to be closed-loop controlled.

Notations: $O_{p\times m}$ and I_m denote respectively the null matrix of dimensions $p\times m$, the identity matrix of dimension m. In order to simplify the notation, the transition matrix $\Phi(t_{k+1},t_k)$ will be denoted $\Phi^{[k]}$. For a symmetric real matrix $S\in\mathbb{R}^{n\times n}$, the notation $S\preceq 0$ ($S\succeq 0$) stands for the negative (positive) semi-definiteness of S.

2. CLASSICAL GLIDESLOPE APPROACH FOR RENDEZVOUS

2.1 Relative motion dynamics

The close range phase of the spacecraft rendezvous mission is characterized by the use of relative navigation since the separation between spacecraft is sufficiently small Fehse (2003). When relative navigation information is available to the chaser, the relative motion of the chaser is expressed in the Local-Vertical-Local-Horizontal (LVLH) frame. The origin of the coordinate frame is located at the center of mass of the leader and the space is spanned by ($\boldsymbol{x}$, $\boldsymbol{y}$, $\boldsymbol{z}$) where the $\boldsymbol{z}$ axis is in the radial direction (R-bar) oriented towards the center of the Earth, the $\boldsymbol{y}$ axis is perpendicular to the leader orbital plane and pointing in the opposite direction of the angular momentum (H-bar) while the $\boldsymbol{x}$ axis completes the right-hand triad $\boldsymbol{x}=\boldsymbol{y}\times\boldsymbol{z}$ (V-bar), see Figure 1. The vector $\boldsymbol{r}$ defines the relative position of the chaser with respect to the target.

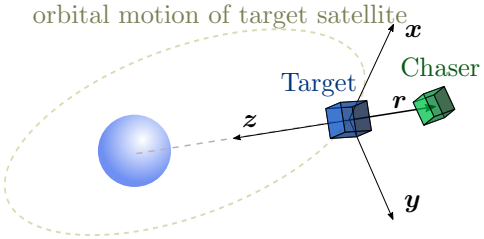

Fig. 1. LVLH frame for spacecraft rendezvous.

Under Keplerian assumptions (no orbital perturbations are considered) and an elliptic reference orbit, the equations of motion for the relative motion in the LVLH frame may be linearized for close separation between the leader and the follower (Alfriend et al., 2010, Chapter 5, Section 5.6.1).

$$\dot{X}(t)=A_0(t)X(t)+\begin{bmatrix}O_{3\times 3}\\ I_3\end{bmatrix}\frac{f(t)}{m_F} \tag{1}$$

where state $X=(x,y,z,dx/dt,dy/dt,dz/dt)^T$ represents positions and velocities in the three fundamental axes of the LVLH frame, $f(t)=[f_x(t)\ f_y(t)\ f_z(t)]^T$ is the thrust vector, m_F is the mass of the follower and the dynamic matrix $A_0(t)$ is a periodic matrix of time t given by :

$$A_0(t)=\begin{bmatrix}0&0&0&1&0&0\\0&0&0&0&1&0\\0&0&0&0&0&1\\a_1(t)&0&\ddot{\nu}&0&0&2\dot{\nu}\\0&a_2(t)&0&0&0&0\\-\ddot{\nu}&0&a_3(t)&-2\dot{\nu}&0&0\end{bmatrix}, \tag{2}$$

and

$$\begin{aligned}a_1(t)&=\dot{\nu}^2-k^4\eta(\nu)^3\\ a_2(t)&=-k^4\eta(\nu)^3\\ a_3(t)&=\dot{\nu}^2+2k^4\eta(\nu)^3\end{aligned}$$

by noting that:

$$\frac{d\nu}{dt}=\frac{n}{(1-e^2)^{3/2}}\underbrace{(1+e\cos\nu)^2}_{\eta(\nu)}=:k^2\eta^2(\nu), \tag{3}$$

where $n=\sqrt{\dfrac{\mu}{a^3}}=2\pi/T$ is the mean motion of the leader orbit, satisfying for any fixed ν_0,t_0:

$$\nu-\nu_0=2\pi\quad\Rightarrow\quad n(t-t_0)=2\pi, \tag{4}$$

and μ is the standard gravitational parameter. It is assumed that only the chaser is active and actuated using 6 ungimbaled identical chemical thrusters. The use of chemical propulsion leads to idealize possible thrusts as impulsive maneuvers providing instantaneous velocity jumps in the three axes while the relative position remains unchanged during firing. The impulsive control input is thus defined as:

$$\Delta v(t_k):=\Delta v_k:=\int_{t_k^-}^{t_k^+}\frac{1}{m_F}\begin{bmatrix}f_x(t)\\f_y(t)\\f_z(t)\end{bmatrix}\mathrm{d}t, \tag{5}$$

where t_k is a generic firing time and Δv_k represents the applied impulsive thrust. In order to compute the transition matrix $\Phi(t,t_0)$ for the linearized equations (1), classical derivations dating back to the seminal publications of Lawden (Lawden, 1963, Chapter 5) and Tschauner-Hempel (Tschauner (1967)) consists in applying a change of independent variable from time t to true anomaly ν and a simplifying coordinate change leading to $\tilde{X}(\nu)=T(\nu)X(t)$ with

$$T(\nu):=\begin{bmatrix}\eta(\nu)I_3 & O_{3\times 3}\\ \eta(\nu)'I_3 & \dfrac{1}{k^2\eta(\nu)}I_3\end{bmatrix}. \tag{6}$$

The obtained simplified autonomous state space representation is expressed as $\tilde{X}'(\nu)=\tilde{A}(\nu)\tilde{X}(\nu)$ where

$$\tilde{A}(\nu)=\begin{bmatrix}0&0&0&1&0&0\\0&0&0&0&1&0\\0&0&0&0&0&1\\0&0&0&0&0&2\\0&-1&0&0&0&0\\0&0&\dfrac{3}{\eta(\nu)}&-2&0&0\end{bmatrix}. \tag{7}$$

Although this state-space equation is linear time-varying, $\tilde{A}(\nu)$ is simple enough to allow for the derivation of the autonomous solution via the computation of a fundamental matrix $\tilde{\varphi}_{\nu_0}(\nu)$ and a transition matrix $\tilde{\Phi}(\nu,\nu_0)$. Based on a particular fundamental solution, the so-called Yamanaka-Ankersen form of the transition matrix, has been proposed in the reference Yamanaka and Ankersen (2002). This form is particularly appealing for computation purposes and therefore the transition matrix $\Phi(t,t_0)$ may be considered as readily computable by:

$$\Phi(t,t_0)=T(\nu)^{-1}\tilde{\varphi}_{\nu_0}(\nu)\tilde{\varphi}_{\nu_0}(\nu_0)^{-1}T(\nu_0). \tag{8}$$

Thus, a controlled trajectory composed of $N+1$ impulses is described by the following equation:

$$X(t)=\Phi(t,t_0)X(t_0)+\sum_{k=0}^{N}\Phi(t,t_k)B\Delta v_k, \tag{9}$$

where $t_1<t_2<\cdots<t_N\leq t$ and Δv_k denotes the impulsive control applied at t_k. $B=[O_{3\times 3}\ I_3]^T$ is the

input matrix. Hereafter, the following notation describing the free motion with a block partitioned transition matrix is adopted:

$$X(t) = \left[\begin{array}{c} \boldsymbol{r}(t) \\ \hline \boldsymbol{v}(t) \end{array}\right] = \left[\begin{array}{c|c} \Phi_{rr}(t,t_0) & \Phi_{rv}(t,t_0) \\ \hline \Phi_{vr}(t,t_0) & \Phi_{vv}(t,t_0) \end{array}\right] \left[\begin{array}{c} \boldsymbol{r}_0 \\ \hline \boldsymbol{v}_0 \end{array}\right] \quad (10)$$

2.2 Hablani's classical glideslope approach

When considering design of impulsive maneuvers for a glideslope rendezvous, the most cited reference is the paper by Hablani et al. (2002) in which the so called classical inbound and outbound glideslope approaches for circular reference are presented in a general setup. Contrasting with this reference, the present paper is restricted to inbound decelerating glideslope trajectories and the main features of the classical glideslope algorithm are now recalled in this particular case. This guidance trajectory is characterized by a straight line and its associated vector $\boldsymbol{\rho}(\nu) = \boldsymbol{r}_c(\nu) - \boldsymbol{r}_T$, defining the commanded path as illustrated by the Figure 2. Defining $\boldsymbol{\rho}_0 = \boldsymbol{r}_0 - \boldsymbol{r}_T$, the unit vector $\boldsymbol{u}$ gives the direction of the straight path:

$$\boldsymbol{u} = \left[\begin{array}{ccc} \dfrac{x_T - x_0}{\|\boldsymbol{\rho}_0\|} & \dfrac{y_T - y_0}{\|\boldsymbol{\rho}_0\|} & \dfrac{z_T - z_0}{\|\boldsymbol{\rho}_0\|} \end{array}\right]^T.$$

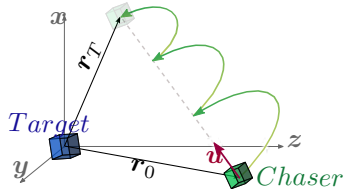

Fig. 2. Glideslope approach.

The chaser is commanded to reach $\boldsymbol{r}_T$ from $\boldsymbol{r}_0$ following a specific commanded profile:

$$\rho(t) = \rho_0 e^{\dfrac{(\dot\rho_0 - \dot\rho_T)t}{\omega\rho_0}} + \frac{\dot\rho_T \rho_0}{\dot\rho_0 - \dot\rho_T}\left(e^{\dfrac{(\dot\rho_0 - \dot\rho_T)t}{\omega\rho_0}} - 1\right), \quad (11)$$

where $\dot\rho_0 < 0$, $\dot\rho_T < 0$ are respectively the initial and final commanded velocities and $\rho_0 = \|\boldsymbol{\rho}_0\|$ is the initial distance to go. These quantities are specified by the designer and inputs for the classical algorithm. Note that $\dot\rho_0 > \dot\rho_T$ and that $\rho_T = 0$ by definition of the trajectory. For a given set of these parameters, the basic principle of the classical algorithm is then to analytically compute a fixed number of impulses equally spaced in time over the transfer duration T. Each computed incremental velocity at $\boldsymbol{r}_k$ is obtained as $\Delta\boldsymbol{v}_k = \boldsymbol{v}_{k_+} - \boldsymbol{v}_{k_-}$ where $\boldsymbol{v}_{k_+}$ is the departure velocity needed to go from $\boldsymbol{r}_k$ to $\boldsymbol{r}_{k+1}$ and $\boldsymbol{v}_{k_-}$ is the arrival velocity at $\boldsymbol{r}_k$. Both quantities are simply obtained by solving the autonomous Hill-Clohessy-Wiltshire equations (Clohessy and Wiltshire (1960)) at each step k.

The classical glideslope algorithm is straightforward and rapid to implement but suffers from key shortcomings. First, it is limited to circular reference orbits. In addition, it is important to mention that the actual trajectory of the chaser will not be strictly along the commanded straight line path but will exhibit humps between the N points where an impulsive maneuver is performed and located on the commanded path (cf. Figure 2). These humps coming from the natural relative motion of the chaser driven by the Hill-Clohessy-Wiltshire equations are nothing but lateral guidance position errors possibly occurring in and out-of-plane that cannot be directly controlled in the classical glideslope algorithm. In addition, if the initial and final commanded velocities of the glideslope profile are *a priori* given, there is no degree of freedom left to control the transfer time and the consumption when $X(0)$ and $X(T)$ are fixed. Indeed, the transfer time T is not fixed *a priori* but deduced from the initial and final commanded velocities $(\dot\rho_0, \dot\rho_T)$ and from the initial distance to go ρ_0:

$$T = \frac{\rho_0}{\dot\rho_0 - \dot\rho_T} \ln\left[\frac{\dot\rho_T}{\dot\rho_0}\right]. \quad (12)$$

The consumption itself is computed *a posteriori* from the velocity increments without any possibility to optimize it for given side conditions of the rendezvous. The objective of the present paper is therefore to propose a new optimization algorithm for the general glideslope framework and extend the results to elliptic reference orbits, taking these two important features into account:

- Minimize the fuel-consumption for a given set of initial and final rendezvous conditions and an *a priori* fixed time of transfer;
- Control the maximum guidance error by defining constraints on the humps profile.

3. MINIMUM-FUEL GLIDESLOPE APPROACH WITH CONTROLLED HUMPS VIA SEMIDEFINITE PROGRAMMING

The main result of the paper is now presented. It mainly consists in deriving a numerically tractable expression for the different constraints on the chaser trajectory and control path to fulfill the second requirement above that will be used in the resulting optimization problem allowing to minimize the fuel consumption during the glideslope transfer. First, the glideslope line tracking constraints are defined according to the transition matrix of the relative linearized keplerian elliptic dynamics. Contrasting with these two references, intermediate positions are free variables and a constraint is added to control the final relative velocity of the chaser. Next, the constraints on the humps profile are dealt with using a parametrization of the relative trajectory defined in Deaconu et al. (2015) and results from polynomial optimization from the reference Nesterov (2000). Finally, a general minimum-fuel multipulse glideslope guidance algorithm relying on the solution of a semidefinite programming problem is proposed.

3.1 Glideslope line tracking

In order to perform the transfer from $\boldsymbol{r}_0$ to $\boldsymbol{r}_T$ in a given duration T, the number of thruster firings is fixed and equal to N. Any two successive impulsive maneuvers are separated by $\Delta t = T/N$ and impulsive thrusts are applied at dates $t_k = k\Delta t$, $k = 0, 1, \cdots, N-1$. The following notation will be used in the rest of the paper.

$$\boldsymbol{r}(t_k) = \boldsymbol{r}_k,\ \rho(t_k) = \rho_k,\ \boldsymbol{v}(t_k) = \boldsymbol{v}_k. \quad (13)$$

Throughout the transfer, the spacecraft must follow the commanded path. After each maneuver, the chaser must be back on the glideslope line. The initial $\boldsymbol{r}_0$ and final $\boldsymbol{r}_N = \boldsymbol{r}_T$ positions are fixed by specifications. Intermediate positions are set free and are parameterized as

$$\boldsymbol{r}_k = \boldsymbol{r}_0 + \rho_k \boldsymbol{u},\ k = 1, \ldots, N-1. \quad (14)$$

The scalars ρ_k are free and denote the travelled distance from $\boldsymbol{r}_0$ to $\boldsymbol{r}_k$. Note that $\rho_0 = 0$ and $\rho_N = \|\boldsymbol{r}_T - \boldsymbol{r}_0\|$. A set of N equations of the form:

$$\boldsymbol{r}_{k+1} = \Phi_{rr}^{[k]} \boldsymbol{r}_k + \Phi_{rv}^{[k]} \boldsymbol{v}_{k_+},\ k = 0, \ldots, N-1, \quad (15)$$

with the position vectors $\boldsymbol{r}_{k+1}$ / $\boldsymbol{r}_k$ as defined above, defines the relative dynamics of the chaser after the

impulsive actuation at t_k. $\boldsymbol{v}_{k_+}$ is the velocity vector right after the impulse is applied. Combining Equations (14) and (15) enforces the requirement for the chaser to come back on the path after each maneuver period leading to the set of equations:

$$\begin{aligned} \rho_{k+1}\boldsymbol{u} - \rho_k \Phi_{rr}^{[k]}\boldsymbol{u} - \Phi_{rv}^{[k]}\boldsymbol{v}_{k_+} &= (\Phi_{rr}^{[k]} - I_3)\boldsymbol{r}_0, \\ \rho_1 \boldsymbol{u} - \Phi_{rv}^{[0]}\boldsymbol{v}_{0_+} &= (\Phi_{rr}^{[0]} - I_3)\boldsymbol{r}_0, \end{aligned} \tag{16}$$

for $k = 1, \cdots, N-1$. Because the reference orbit is considered to be elliptic, the transition matrix is not constant all over the orbit and need to be updated for each maneuver. Since time intervals for impulse control are input data, all transition matrices $\Phi^{[k]}$ can be computed *a priori*. The decision variables in (16) are composed by the sequence of scalar variables ρ_k for $k = 1, \cdots, N-1$ and by the sequence of vectors $\boldsymbol{v}_{k_+}$ for $k = 0, 1, \cdots, N-1$. The sequence of impulses is deduced afterwards, computing the difference between the design variable $\boldsymbol{v}_{k_+}$ and the velocity vector $\boldsymbol{v}_{k_-}$ resulting from the previous maneuver and from the relative dynamics of the chaser:

$$\boldsymbol{v}_{k+1_-} = \Phi_{vr}^{[k]} r_k + \Phi_{vv}^{[k]}\boldsymbol{v}_{k_+}, \; k = 0, 1, \cdots, N-1. \tag{17}$$

Therefore, we have

$$\Delta \boldsymbol{v}_k = \boldsymbol{v}_{k_+} - \boldsymbol{v}_{k_-}. \tag{18}$$

3.2 Final velocity constraint

Since a last impulse is needed to control the final velocity of the spacecraft, an additional equality constraint is defined. This $(N+1)^{th}$ impulse maneuver is given by

$$\begin{aligned} &\Delta \boldsymbol{v}_N = \boldsymbol{v}_{N_+} - \boldsymbol{v}_{N_-}, \\ &\Delta \boldsymbol{v}_N = \boldsymbol{v}_{N_+} - \Phi_{vr}^{[N-1]}\boldsymbol{r}_{N-1} - \Phi_{vv}^{[N-1]}\boldsymbol{v}_{N-1_+}. \end{aligned} \tag{19}$$

Setting the vector $\boldsymbol{v}_{N_+} = \boldsymbol{v}_T$ as the desired final velocity and $\Delta \boldsymbol{v}_N$ being a free variable, an extra equality constraint is appended:

$$\boldsymbol{v}_T - \Phi_{vr}^{[N-1]}\boldsymbol{r}_0 = \Phi_{vr}^{[N-1]}\boldsymbol{u}\rho_{N-1} + \Phi_{vv}^{[N-1]}\boldsymbol{v}_{N-1_+} + \Delta \boldsymbol{v}_N. \tag{20}$$

As mentioned earlier, $\Delta \boldsymbol{v}_N$, ρ_{N-1} and $\boldsymbol{v}_{N-1_+}$ are the only free variables of (20).

3.3 Constraints on guidance error

The aim of this subsection is to give a numerically tractable formulation of the continuous constraints imposed on the spacecraft relative trajectory in order to bound the guidance error inherent to the impulsive glideslope approach. In the spirit of the method developed in Deaconu et al. (2015), the idea is to look for an equivalent finite description of the admissible relative trajectories using various tools from algebraic geometry and in particular, properties of non-negative polynomials. The main steps of the method are: 1) define a piecewise linear envelope enclosing the admissible trajectory; 2) use a rational parametrization of the trajectory between each pulse to transform the previous continuous linear constraints into polynomials non negativity constraints; 3) apply representation theorems of cones of nonnegative polynomials from Nesterov (2000) to get a final semidefinite formulation of the constraints on guidance error.

First, a set of linear constraints on the chaser's relative trajectory is defined, for each maneuver, by:

$$A_k \boldsymbol{r}(t) \leq b_k, \; \forall t \in [t_k \; t_{k+1}], \; \forall k = \{0, \ldots, N-1\}. \tag{21}$$

The interval $[t_k \; t_{k+1}]$ corresponds to the maneuver period, from the $(k+1)^{\text{th}}$ impulse to the instant when the spacecraft is back on the glideslope line. $A_k \in \mathbb{R}^{n_c \times 3}$ is a constant matrix and $b_k \in \mathbb{R}^{n_c}$ is a constant vector. These matrices are built from input specifications related to the maximal allowable excursion. n_c denotes the number of scalar inequalities, each of which defines a plane bounding the trajectory. For instance, let define vectors u_1 and u_2 as an orthonormal basis for the null space of $\boldsymbol{u}^T$. By choosing

$$A_0 = \begin{bmatrix} u_1^T \\ -u_1^T \\ u_2^T \\ -u_2^T \end{bmatrix} \text{ and } b_0 = \begin{bmatrix} u_1^T(r_0 + \delta_1 u_1) \\ -u_1^T(r_0 - \delta_1 u_1) \\ u_2^T(r_0 + \delta_2 u_2) \\ -u_2^T(r_0 - \delta_2 u_2) \end{bmatrix}, \tag{22}$$

a rectangular corridor with four planes parallel to the glideslope direction is defined. Parameters δ_1 and δ_2 specify the distance from the glideslope line to each pair of planes. In this case, $n_c = 4$ and the matrix $A_k = A_0$ is identical $\forall k = \{0, \ldots, N-1\}$. Vector b_k is changing with the different distance specifications $\{\delta_{1_k}, \delta_{2_k}\}$ associated to each maneuver. Applying the change of variable (6) to the general constraint (21), we get:

$$\begin{aligned} A_k \tilde{\boldsymbol{r}}(\nu) \leq \; & \eta(\nu) b_k, \; \forall \nu \in [\nu_k \; \nu_{k+1}], \\ & \forall k = \{0, \ldots, N-1\}. \end{aligned} \tag{23}$$

In Deaconu et al. (2015), the autonomous relative trajectory was parameterized as follows,

$$\begin{cases} \tilde{x}(\nu) = (2 + e\cos\nu)(d_1 \sin\nu - d_2 \cos\nu) + d_3 \\ \qquad\quad +3 d_4 J(\nu, \nu_0)(1 + e\cos\nu)^2, \\ \tilde{y}(\nu) = d_5 \cos\nu + d_6 \sin\nu, \\ \tilde{z}(\nu) = (1 + e\cos\nu)(d_2 \sin\nu + d_1 \cos\nu) \\ \qquad\quad -3\, e\, d_4 J(\nu, \nu_0) \sin\nu (1 + e\cos\nu) + 2 d_4, \end{cases} \tag{24}$$

for $\nu \in [\nu_0, \nu_f]$, where the vector of parameters D is defined by (26) and depends linearly on the initial state, the integral term $J(\nu, \nu_0)$ is given by

$$J(\nu, \nu_0) = \int_{\nu_0}^{\nu} \frac{1}{\eta(u)^2} du = \frac{n}{(1-e^2)^{3/2}}(t - t_0). \tag{25}$$

We are now in a position to apply the following change of variable in order to transform the trigonometrical functions into rational functions

$$w = \tan\frac{\nu}{2}, \; \cos\nu = \frac{1 - w^2}{1 + w^2}, \; \sin\nu = \frac{2w}{1 + w^2}. \tag{27}$$

The propagation of the spacecraft relative motion can then be expressed as a function of w:

$$\begin{cases} \tilde{x}(w) = \dfrac{1}{(1+w^2)^2}\Big[P_x(w) + 3 d_4 P_{Jx}(w) J(w)\Big], \\ \tilde{y}(w) = \dfrac{1}{(1+w^2)} P_y(w), \\ \tilde{z}(w) = \dfrac{1}{(1+w^2)^2}\Big[P_z(w) + 2 d_4 P_{Jz}(w) J(w)\Big] \end{cases} \tag{28}$$

for $w \in [w_0, w_f]$. Only the term with $J(w)$ is non-rational and requires to be dealt with. All P_* functions are polynomials:

$$\begin{aligned} &P_{Jx}(w) = \Big((1+e) + (1-e)w^2\Big)^2, \\ &P_{Jz}(w) = -3e\Big((1+e)w + (1-e)w^3\Big), \\ &P_x(w) = \sum_{i=0}^{4} p_{xi} w^i, \; P_y(w) = \sum_{i=0}^{2} p_{yi} w^i, \; P_z(w) = \sum_{i=0}^{4} p_{zi} w^i \end{aligned} \tag{29}$$

where coefficients of P_x, P_y and P_z depend linearly on the vector D

$$\underbrace{\begin{bmatrix} d_1 \\ d_2 \\ d_3 \\ d_4 \\ d_5 \\ d_6 \end{bmatrix}}_{D} = \underbrace{\left[\begin{array}{ccc|ccc} 0 & 0 & \frac{3(e+\cos\nu_0)}{e^2-1} & -\frac{2\cos\nu_0+e\cos^2\nu_0+e}{e^2-1} & 0 & \frac{\sin\nu_0(1+e\cos\nu_0)}{e^2-1} \\ 0 & 0 & \frac{3\sin\nu_0(1+e\cos\nu_0+e^2)}{(e^2-1)(1+e\cos\nu_0)} & -\frac{\sin\nu_0(2+e\cos\nu_0)}{e^2-1} & 0 & -\frac{\cos\nu_0+e\cos^2\nu_0-2e}{e^2-1} \\ 1 & 0 & -\frac{3e\sin\nu_0(2+e\cos\nu_0)}{(e^2-1)(1+e\cos\nu_0)} & \frac{e\sin\nu_0(2+e\cos\nu_0)}{e^2-1} & 0 & \frac{e^2\cos^2\nu_0+e\cos\nu_0-2}{e^2-1} \\ 0 & 0 & -\frac{3e\cos\nu_0+e^2+2}{e^2-1} & \frac{(1+e\cos\nu_0)^2}{e^2-1} & 0 & -\frac{e\sin\nu_0(1+e\cos\nu_0)}{e^2-1} \\ 0 & \cos\nu_0 & 0 & 0 & -\sin\nu_0 & 0 \\ 0 & \sin\nu_0 & 0 & 0 & \cos\nu_0 & 0 \end{array}\right]}_{C(\nu_0)} \underbrace{\begin{bmatrix} \tilde{\boldsymbol{r}}_0 \\ \tilde{\boldsymbol{v}}_0 \end{bmatrix}}_{\tilde{X}(\nu_0)} \tag{26}$$

$$\underbrace{\begin{bmatrix} p_{x0} \\ p_{x1} \\ p_{x2} \\ p_{x3} \\ p_{x4} \end{bmatrix}}_{p_x} = \underbrace{\begin{bmatrix} 0 & -2-e & 1 & 0 & 0 & 0 \\ 4+2e & 0 & 0 & 0 & 0 & 0 \\ 0 & 2e & 2 & 0 & 0 & 0 \\ 4-2e & 0 & 0 & 0 & 0 & 0 \\ 0 & 2-e & 1 & 0 & 0 & 0 \end{bmatrix}}_{C_x} D, \tag{30}$$

$$\underbrace{\begin{bmatrix} p_{y0} \\ p_{y1} \\ p_{y2} \end{bmatrix}}_{p_y} = \underbrace{\begin{bmatrix} 0 & 0 & 0 & 0 & 1 & 0 \\ 0 & 0 & 0 & 0 & 0 & 2 \\ 0 & 0 & 0 & 0 & -1 & 0 \end{bmatrix}}_{C_y} D, \tag{31}$$

$$\underbrace{\begin{bmatrix} p_{z0} \\ p_{z1} \\ p_{z2} \\ p_{z3} \\ p_{z4} \end{bmatrix}}_{p_z} = \underbrace{\begin{bmatrix} e+1 & 0 & 0 & 2 & 0 & 0 \\ 0 & 2e+2 & 0 & 0 & 0 & 0 \\ -2e & 0 & 0 & 4 & 0 & 0 \\ 0 & 2-2e & 0 & 0 & 0 & 0 \\ e-1 & 0 & 0 & 2 & 0 & 0 \end{bmatrix}}_{C_z} D. \tag{32}$$

Before defining trajectory constraints, we first need to deal with the integral term $J(\nu, \nu_0)$ in the spacecraft relative motion (28). In order to have a rational expression for the motion, a polynomial approximation is derived to bound J over $w \in [w_0, w_f]$:

$$J(w) = \Theta_r(w) + \varepsilon(w) \Rightarrow \underbrace{\Theta_r(w) - \bar{\varepsilon}}_{\Theta_l(w)} \leq J(w) \leq \underbrace{\Theta_r(w) + \bar{\varepsilon}}_{\Theta_u(w)} \tag{33}$$

where $\Theta_r(w)$ is a polynomial of degree r and $\bar{\varepsilon}$ the maximum error due to the approximation.

The linear constraints (23) are transformed by the change of variables (27) into

$$A_k \tilde{\boldsymbol{r}}(w) \leq \left(\frac{1+e+(1-e)w^2}{1+w^2}\right) b_k, \ \forall w \in [w_k \ w_{k+1}], \ \forall k = \{0, \ldots, N-1\}, \tag{34}$$

with $w_k = \tan(\nu_k/2)$. Let us expand the i^{th} row of this latter expression:

$$A_{k_{i1}} \tilde{x}(w) + A_{k_{i2}} \tilde{y}(w) + A_{k_{i3}} \tilde{z}(w) \leq \left(\frac{1+e+(1-e)w^2}{1+w^2}\right) b_{k_i}, \tag{35}$$

that is equivalent to

$$\frac{\Gamma_i^k(w)}{(1+w^2)^2} \geq 0, \tag{36}$$

with

$$\begin{aligned} \Gamma_i^k(w) = b_{k_i}\Big(\Big(1+w^2)(1+e+(1-e)w^2\Big)\Big) \\ -A_{k_{i1}}\Big[P_x(w) + 3d_4 P_{Jx}(w) J(w)\Big] \\ -A_{k_{i2}}(1+w^2) P_y(w) \\ -A_{k_{i3}}\Big[P_z(w) + 2d_4 P_{Jz}(w) J(w)\Big]. \end{aligned} \tag{37}$$

Replacing the function $J(w)$ by the two extreme bounding polynomials Θ_l and Θ_u, the above function becomes polynomial, respectively Γ_{il}^k and Γ_{iu}^k. Hence, the inequality (36) becomes a pair of inequalities with Γ_{il}^k and Γ_{iu}^k, that must be repeated for each constraint i (rows of A_k) and for each maneuver k. Finally, the whole constraint on the guidance error is formulated as the polynomial non negativity constraints:

$$\begin{cases} \Gamma_{il}^k(w) \geq 0, \\ \Gamma_{iu}^k(w) \geq 0, \end{cases} \tag{38}$$

for $i = \{1, \ldots, n_c\}$, for $k = \{0, \ldots, N-1\}$, $\forall w \in [w_k \ w_{k+1}]$, with

$$\begin{aligned} \Gamma_{il}^k(w) = b_{k_i}\Big(\Big(1+w^2)(1+e+(1-e)w^2\Big)\Big) \\ -A_{k_{i1}}\Big[P_x(w) + 3d_4 P_{Jx}(w) \Theta_l(w)\Big] \\ -A_{k_{i2}}(1+w^2) P_y(w) \\ -A_{k_{i3}}\Big[P_z(w) + 2d_4 P_{Jz}(w) \Theta_l(w)\Big], \\ \Gamma_{iu}^k(w) = b_{k_i}\Big(\Big(1+w^2)(1+e+(1-e)w^2\Big)\Big) \\ -A_{k_{i1}}\Big[P_x(w) + 3d_4 P_{Jx}(w) \Theta_u(w)\Big] \\ -A_{k_{i2}}(1+w^2) P_y(w) \\ -A_{k_{i3}}\Big[P_z(w) + 2d_4 P_{Jz}(w) \Theta_u(w)\Big]. \end{aligned} \tag{39}$$

The properties of non negative polynomials and representation theorems of cones of non negative polynomials given in Nesterov (2000) allow us to translate these inequalities defined on an infinite interval into a semi-definite programming problem:

$$\begin{cases} \exists \ Y_{1il}^k, Y_{2il}^k \succeq 0 \ \text{ s.t. } \gamma_{il}^k = \Lambda^*(Y_{1il}^k, Y_{2il}^k), \\ \exists \ Y_{1iu}^k, Y_{2iu}^k \succeq 0 \ \text{ s.t. } \gamma_{iu}^k = \Lambda^*(Y_{1iu}^k, Y_{2iu}^k), \end{cases} \tag{40}$$

for $i = \{1, \ldots, n_c\}$, for $k = \{0, \ldots, N-1\}$. Γ_{il}^k and Γ_{iu}^k are represented by their vector of coefficients γ_{il}^k and γ_{iu}^k, respectively. The exact definition of the linear operator Λ^* is omitted here for the sake of conciseness but it may be

obtained in the appendix of the reference Deaconu et al. (2015).

3.4 Definition of the Cost function

Apart from the control of the humps during the glideslope, the other main objective of the approach is to minimize the fuel consumption during the transfer. As 6 ungimbaled identical chemical thrusters are used, the cost function may be naturally defined as the 1-norm of the $N+1$ impulsive thrusts:

$$C(N) = \sum_{k=0}^{N} \|\Delta \boldsymbol{v}_k\|_1, \tag{41}$$

with $\Delta \boldsymbol{v}_k = \boldsymbol{v}_{k_+} - \boldsymbol{v}_{k_-}$. The formulation (41) is transformed in order to express the above criterion with respect to the decision variables variables $\boldsymbol{v}_{k_+}$, $k = 0, \cdots, N-1$, ρ_k, $k = 1, \cdots, N-1$ and Δv_N:

$$\begin{aligned} C(N) = & \|\boldsymbol{v}_{0_+} - \boldsymbol{v}_{0_-}\|_1 + \\ & \sum_{k=1}^{N-1} \|\boldsymbol{v}_{k_+} - \Phi_{vr}^{[k-1]}(r_0 + \rho_{k-1}u) - \Phi_{vv}^{[k-1]}\boldsymbol{v}_{k-1_+}\|_1 \\ & + \|\Delta \boldsymbol{v}_N\|_1, \end{aligned} \tag{42}$$

where $\boldsymbol{v}_{0_-}$ is the initial velocity vector. This cost function involving absolute values can be transformed into a linear function with the introduction of new variables and inequality constraints:

$$\begin{aligned} \boldsymbol{v}_{0_+} - \boldsymbol{v}_{0_-} &\leq \alpha_0 \\ -\left(\boldsymbol{v}_{0_+} - \boldsymbol{v}_{0_-}\right) &\leq \alpha_0 \\ \boldsymbol{v}_{k_+} - \Phi_{vr}^{[k-1]}(r_0 + \rho_{k-1}u) - \Phi_{vv}^{[k-1]}\boldsymbol{v}_{k-1_+} &\leq \alpha_k \\ -\left(\boldsymbol{v}_{k_+} - \Phi_{vr}^{[k-1]}(r_0 + \rho_{k-1}u) - \Phi_{vv}^{[k-1]}\boldsymbol{v}_{k-1_+}\right) &\leq \alpha_k \\ \Delta \boldsymbol{v}_N &\leq \alpha_N \\ -\Delta \boldsymbol{v}_N &\leq \alpha_N \end{aligned} \tag{43}$$

where α_k are extra decision variables, and the cost function becomes:

$$C(N) = \sum_{k=0}^{N} [1 \ 1 \ 1]\, \alpha_k$$

3.5 A semidefinite programming problem

Having defined all the different ingredients in the previous subsections, the last step consists in gathering them in a compact formulation. Therefore, a solution to the initial minimum-fuel glideslope guidance problem may be obtained via the solution of the following semidefinite programming problem.

$$\begin{aligned} &\min \ c^T \alpha \\ &\text{s.t.} \\ &\rho_{k+1}u - \rho_k \Phi_{rr}^{[k]} u - \Phi_{rv}^{[k]} \boldsymbol{v}_{k_+} = (\Phi_{rr}^{[k]} - I_3)\boldsymbol{r}_0, \ k = 1, \ldots, N-1, \\ &\rho_1 u - \Phi_{rv}^{[0]} \boldsymbol{v}_{0_+} = (\Phi_{rr}^{[0]} - I_3)\boldsymbol{r}_0, \\ &\boldsymbol{v}_T - \Phi_{vr}^{[N-1]} \boldsymbol{r}_0 = \Phi_{vr}^{[N-1]} u \rho_{N-1} + \Phi_{vv}^{[N-1]} \boldsymbol{v}_{N-1_+} + \Delta \boldsymbol{v}_N, \\ &\alpha_0 \geq \boldsymbol{v}_{0_+} - \boldsymbol{v}_{0_-}, \\ &\alpha_0 \geq -\left(\boldsymbol{v}_{0_+} - \boldsymbol{v}_{0_-}\right), \\ &\alpha_k \geq \left(\Phi_{vr}^{[k-1]}(\rho_{k-1}u + r_0) + \Phi_{vv}^{[k-1]} \boldsymbol{v}_{k-1_+} - \boldsymbol{v}_{k_+}\right), \\ &\alpha_k \geq \boldsymbol{v}_{k_+} - \Phi_{vr}^{[k-1]}(\rho_{k-1}u + r_0) - \Phi_{vv}^{[k-1]} \boldsymbol{v}_{k-1_+}, \ k = 1, \ldots, N-1, \\ &\alpha_N \geq \Delta \boldsymbol{v}_N, \\ &\alpha_N \geq -\Delta \boldsymbol{v}_N, \\ &\gamma_{il}^k = \Lambda^*(Y_{1il}^k, Y_{2il}^k), \ i = \{1, \ldots, n_c\}, \ k = \{0, \ldots, N-1\}, \\ &\gamma_{iu}^k = \Lambda^*(Y_{1iu}^k, Y_{2iu}^k), \\ &Y_{1il}^k \succeq 0, \ Y_{2il}^k \succeq 0, \\ &Y_{1iu}^k \succeq 0, \ Y_{2iu}^k \succeq 0, \end{aligned} \tag{44}$$

with $c = [1 \ \ldots \ 1]^T$ and $\alpha = \left[\alpha_0^T \ \ldots \ \alpha_N^T\right]^T$. When considering a second order polynomial approximation, we have that $Y_{1il}^k \in \mathbb{R}^{4\times4}$, $Y_{2il}^k \in \mathbb{R}^{3\times3}$, $Y_{1iu}^k \in \mathbb{R}^{4\times4}$ and $Y_{2iu}^k \in \mathbb{R}^{3\times3}$. Vectors γ_{il}^k and γ_{iu}^k are the given vector of coefficients of polynomials Γ_{il}^k and Γ_{iu}^k. n_c is the number of row of matrix A_k. Decision variables are

- α_k for $k = \{0, \ldots, N\}$,
- ρ_k for $k = \{1, \ldots, N-1\}$,
- $\boldsymbol{v}_{k_+}$ for $k = \{0, \ldots, N-1\}$,
- $\Delta \boldsymbol{v}_N$,
- Y_{1il}^k, Y_{2il}^k, Y_{1iu}^k and Y_{2iu}^k for $i = \{1, \ldots, n_c\}$, for $k = \{0, \ldots, N-1\}$.

4. NUMERICAL SIMULATION

4.1 Example 1

First, an illustration based on PRISMA Berges et al. (2007) is presented. PRISMA programme is a cooperative effort between the Swedish National Space Board (SNSB), the French Centre National d'Etudes Spatiales (CNES), the German Deutsche Zentrum für Luft- und Raumfahrt (DLR) and the Danish Danmarks Tekniske Universitet (DTU) Larsson et al. (2006). Launched on June 15, 2010 Yasny (Russia), it was intended to test in-orbit new guidance schemes (particularly autonomous orbit control) for formation flying and rendezvous technologies. The orbital elements of the target orbit, as well as initial and final rendezvous conditions, are listed in Table 1.

Semi-major axis	$a = 7011$ km
Inclination	$i = 98$ deg.
Argument of Perigee	$\omega = 0$ deg.
RAAN	$\Omega = 190$ deg.
Eccentricity	$e = 0.004$
True Anomaly	$\nu_0 = 0$ rad.
t_0	0 s
$X_0^T = [r_0^T \ v_{0_-}^T]$	$[-400 \ 40 \ -50 \ -0.5 \ 0 \ 0]$ m -m/s
T	1500 s
$X_T^T = [r_T^T \ v_T^T]$	$[-40 \ 0 \ -10 \ 0 \ 0 \ 0]$ m -m/s
N	6

Table 1. PRISMA rendezvous characteristics

In this first example, the target evolves on a quasi-circular orbit and the standard glideslope approach is employed to transfer the chaser from $\boldsymbol{r}_0$ to $\boldsymbol{r}_T$ in 6 maneuvers (N)

during 25 min ($T = 1500$ s). Three algorithms are compared: the classical one from Hablani et al. (2002) based on Hill-Clohessy-Wiltshire equations, its direct extension based on Yamanaka-Ankersen equations and the proposed optimal glideslope algorithm. In all cases, the resulting impulsive control sequence $\Delta \boldsymbol{v}_i$ is applied and propagated with the Tschauner-Hempel equations. We aim at emphasizing the significant drift induced when using the glideslope control computed with the Hill-Clohessy-Wiltshire equations even when the reference orbit is quasi-circular. Figure 3 shows the chaser trajectories for the different approaches. The final position of the chaser resulting from the Hablani's glideslope is $[-49.2, -0.2, -16]$ m, that is 11m away from the desired position. Regarding the velocity profile along the glideslope, the relevant parameters are set such that $\dot{\rho}_0 = -1$ and $\dot{\rho}_T$ is imposed by the maneuver period T. The global consumptions of the standard circular and elliptic glideslope algorithms are similar and given respectively by 2.9705 m/s and 2.977 m/s. The specifications for the proposed algorithm are defined by a final velocity $\boldsymbol{v}_T = \boldsymbol{0}$ m/s and a constraint on the trajectory characterized by a 10 m $\times$10 m corridor. The consumption obtained is 1.9698 m/s which is much lower than the standard approach.

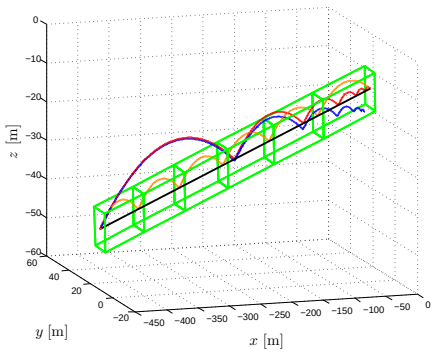

Fig. 3. *Chaser relative trajectories, standard circular glideslope (blue) vs. elliptic glideslope (red) vs. proposed optimal algorithm (orange).*

The sequences of impulsive maneuvers for the standard elliptic glideslope and the minimum-fuel algorithm are detailed below in Table 2 and depicted in Figure 4. Note also that the standard trajectories do not respect the admissible corridor in green.

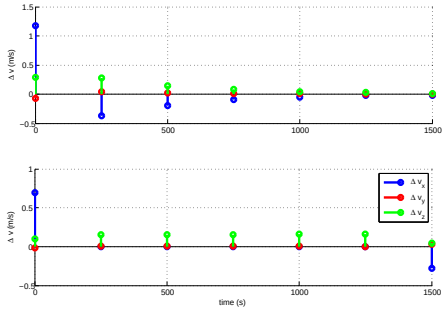

Fig. 4. *Impulsive control sequences for the standard elliptic glideslope (top) and for the optimal glideslope (bottom) in example 1.*

4.2 Example 2

In this second example, the standard elliptic glideslope approach as it may be built from the information obtained

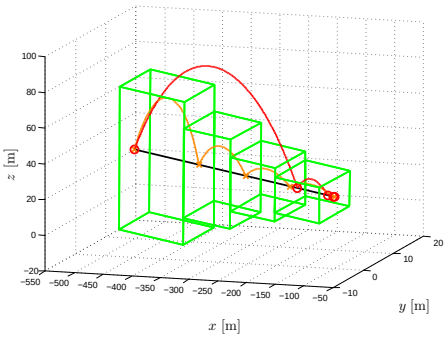

Fig. 5. *Chaser relative trajectories: standard elliptic glideslope algorithm (red) vs. proposed optimal algorithm (orange).*

in Okasha and Newman (2011) and the proposed optimal algorithm are compared in a case for which the eccentricity of the reference orbit is high. The parameters defining the conditions of the rendezvous are set as follows:

$$T = 540 \text{ s},\ N = 4,\ n = 0.001 \text{ rad/s},\ e = 0.7,\ \boldsymbol{v}_T = \boldsymbol{0},$$

$$\boldsymbol{r}_0 = \begin{bmatrix} -500 \\ 10 \\ 30 \end{bmatrix} \text{m},\ \boldsymbol{r}_T = \begin{bmatrix} -100 \\ 0 \\ 20 \end{bmatrix} \text{m},\ \boldsymbol{v}_{0\_} = \begin{bmatrix} 0 \\ 0 \\ 0.5 \end{bmatrix} \text{m/s}.$$

Regarding the constraints on the trajectory guidance error, we define for each maneuver a box (or a corridor) defined by 4 planes with (22). Thus, 4 boxes centered around the glideslope line are defined:

maneuver	1	2	3	4
height [m]	90	50	30	20
width [m]	10	10	10	10

Figure 5 depicts the chaser trajectories for the two methods and where the four boxes corresponding to trajectory constraints are represented in green. The consumption of the standard glideslope algorithm is 7.74 m/s whereas the consumption of our optimal algorithm is 4.53 m/s. The respective sequences of impulsive maneuvers are presented in Table 3 and depicted in Figure 6.

time (s)	0	135	270	405	540
standard glideslope					
Δv_x (m/s)	2.2830	-1.5736	-0.3350	-0.0669	-0.0165
Δv_y (m/s)	-0.0512	0.0544	0.0095	0.0017	0.0004
Δv_z (m/s)	1.3608	1.6940	0.2323	0.0486	0.0114
optimal glideslope					
Δv_x (m/s)	0.9751	0	0	0	-0.6517
Δv_y (m/s)	-0.0129	0.0168	0.0039	0.0009	0.0165
Δv_z (m/s)	0.5938	1.2648	0.5613	0.3079	0.1267

Table 3. *Impulsive control sequences for ex. 2.*

5. CONCLUSION

In this paper, a new algorithm based on semidefinite programming has been proposed for the problem of impulsive close range glideslope rendezvous in an elliptic orbit. The two main shortcomings (the lack of control on the bounds over the inherent guidance errors and the impossibility of minimizing the fuel consumption) of the classical algorithm by Hablani et al. (2002) are tackled via a combination of simple techniques mainly borrowed from the field of non negative polynomials theory. The main design feature included in the new proposed glideslope algorithm is the possibility to specify an admissible volume for each hump of the relative trajectory and therefore to control the guidance error all along the rectilinear

time (s)	0	250	500	750	1000	1250	1500
standard glideslope							
Δv_x (m/s)	1.1784	-0.3757	-0.1915	-0.0976	-0.0498	-0.0254	-0.0245
Δv_y (m/s)	-0.0749	0.0455	0.0231	0.0117	0.0058	0.0029	0.0028
Δv_z (m/s)	0.2879	0.2779	0.1455	0.0780	0.0436	0.0261	0.0083
optimal glideslope							
Δv_x (m/s)	0.6930	0	0	0	0	0	-0.2785
Δv_y (m/s)	-0.0173	0.0087	0.0068	0.0048	0.0027	0.0004	0.0312
Δv_z (m/s)	0.0979	0.1525	0.1543	0.1560	0.1577	0.1595	0.0486

Table 2. *Impulsive control sequences for ex. 1.*

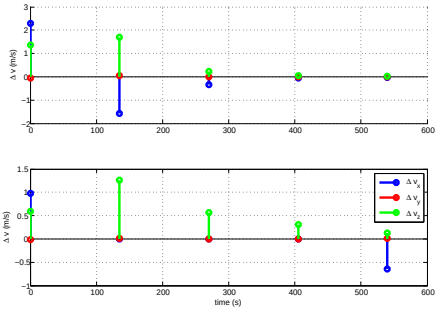

Fig. 6. *Impulsive control sequences for the standard glideslope (top) and for the optimal glideslope (bottom) in example 2.*

path. Two different examples have clearly shown the key features of the exposed results like a significant improved fuel consumption with respect to Hablani's algorithm and a user-defined bound profile on the maximum guidance error, which turns out to be very useful when dealing with visibility constraints while keeping a reasonable numerical complexity of computation.

6. ACKNOWLEDGEMENTS

The Authors would like to thank Jean-Claude Berges from CNES and Damiana Losa from Thales Alenia Space for the grants that partly supports this activity.

REFERENCES

Alfriend, K., Vadali, S., Gurfil, P., How, J., and Breger, L. (2010). *Spacecraft Formation Flying: Dynamics, Control and Navigation*. Astrodynamics Series. Elsevier, Burlington, MA, USA.

Ariba, Y., Arzelier, D., Urbina Iglesias, L.S., and Louembet, C. (2016). V-bar and r-bar glideslope guidance algorithms for fixed-time rendre-vous: a linear programming approach. In *IFAC Symposium on Automatic Control in Aerospace (ACA)*. Sherbrooke (Canada).

Berges, J.C., Cayeux, P., Gaudel-Vacaresse, A., and Meyssignac, B. (2007). Cnes approaching guidance experiment on ffiord. In *20th. International Symposium on Space Flight Dynamics*. Annapolis, Maryland, USA.

Clohessy, W. and Wiltshire, R. (1960). Terminal guidance system for satellite rendezvous. *Journal of the Astronautical Sciences*, 27(9), 653–658.

Deaconu, G., Louembet, C., and Théron, A. (2015). Designing continuously constrained spacecraft relative trajectories for proximity operations. *Journal of Guidance, Control, and Dynamics*, 38(7), 1208–1217.

Fehse, W. (ed.) (2003). *Automated rendezvous and docking of spacecraft*. Cambridge Aerospace Series. Cambridge University Press, Cambridge, UK.

Hablani, H., Tapper, M., and David J. Dana-Bashian, D. (2002). Guidance and relative navigation for autonomous rendezvous in a circular orbit. *Journal of Guidance, Control and Dynamics*, Vol. 25(No. 3).

Larsson, R., Berge, S., Bodin, P., and Jönsson, U. (2006). Fuel efficient relative orbit control stategies for formation flying and rendezvous within prisma. In 29^{th} *Annual AAs Guidance and Control Conference*. Breckenridge, Colorado, USA.

Lawden, D. (1963). *Optimal trajectories for space navigation*. Butterworth, London, England.

Nesterov, Y. (2000). Squared functionals systems and optimization problems. In H. Frenck, K. Roos, T. Terlaky, and S. Zhang (eds.), *High Performance Optimization*, chapter 17, 405–440. Springer US, Boston, MA, USA.

Okasha, M. and Newman, B. (2011). Guidance, navigation and control for satellite proximity operations using tschauner-hempel equations. In *AIAA Guidance, Navigation and Control Conference*. Portland, Oregon, USA.

Pearson, D. (1989). The glideslope approach. *Advances in Astronautical Sciences*, 69, 109–123.

Tschauner, J. (1967). Elliptic orbit rendezvous. *AIAA Journal*, 5(6), 1110–1113.

Wang, F., Cao, X., and Chen, X. (2007). Guidance algorithms for the near-distance rendezvous of on-orbit-servicing spacecraft. *Transactions of Japanese Society for Aeronautical and Space Sciences*, 50(167), 9–17.

Yamanaka, K. and Ankersen, F. (2002). New state transition matrix for relative motion on an arbitrary elliptical orbit. *Journal of Guidance, Control, and Dynamics*, 25, 60–66.